Follow-Up Imaging of Soft Tissue Tumors

26

Johan L. Bloem and Carla S.P. Van Rijswijk

Contents

J.L. Bloem (✉) • C.S.P. Van Rijswijk
Department of Radiology,
Leiden University Medical Center (LUMC),
Gebouw 1., Postbus 9600, 2300 RC,
Leiden, The Netherlands
e-mail: j.l.bloem@lumc.nl

26.1 Introduction

The aim of therapy in patients with soft tissue sarcoma is to irradicate (curative) or modify biologic behavior (palliative) of sarcoma while minimizing damage of normal tissues. This is done by local (surgery, isolated limb perfusion, and radiation) or systemic (neoadjuvant and adjuvant chemotherapy) therapy. Prognosis of patients with soft tissue sarcoma is mainly influenced by local recurrence and development of distant metastasis and thus also by response to treatment [1]. Approximately one-third of all patients with soft tissue sarcomas will develop local recurrence or distant metastatic disease, with the highest risk in the first few years after treatment; however, late recurrences after 5 years do occur [2–4]. The overall survival mainly depends on the development of metastatic disease.

The patterns of recurrence vary with the anatomic site of the primary tumor [5]. Patients with extremity and superficial trunk primaries have a higher predilection for metastases and a lower probability of locoregional recurrences. In contrast, patients with retroperitoneal or head and neck tumors have a higher tendency toward locoregional recurrences compared to metastases. In this chapter we'll address several topics related to therapy. After a brief discussion on therapy-induced changes in normal tissue, which is important in diagnosing recurrence, we'll

address monitoring the response to treatment, imaging locoregional recurrence, and finally diagnosis of metastases.

26.2 Therapy-Induced Changes in Normal Tissue

Surgery, radiation therapy, isolated limb perfusion, systemic chemotherapy, angiogenesis-inhibiting drugs, therapy- and cancer-induced cachexia, and supportive therapy such as blood transfusions, erythropoietin (Epo), corticosteroids, growth colony stimulating factor (G-CSF), and peripheral stem cell transplantation may all cause acute and/or chronic reversible or irreversible changes in normal tissue. These changes are often seen on imaging during and/or following therapy and need to be differentiated from residual or recurrent tumor and metastatic disease. These changes include edema, avascular necrosis, mucoid degeneration, serous atrophy, osteopenia, regeneration or reconversion of hematopoietic marrow, extramedullary hematopoieses, hematoma, seroma, denervation of muscle, and therapy-induced cancers. Most diagnostic problems related to these therapy effects occur in the bone marrow of patients with osseous tumors. Bone marrow changes do occur in patients with soft tissue tumors but then pose less of a diagnostic problem. In this chapter we'll limit the discussion to changes that may cause diagnostic problems in patients with soft tissue tumors.

Various soft tissue tumors such as neurofibromatosis and giant cell tumors are treated with biologicals such as imatinib (Gleevec). In these patients extensive bone marrow changes displaying low signal intensity on T1-weighted MR images and high signal intensity on fluid-sensitive MR sequences may be seen. These may progress during treatment and may completely disappear following cessation of treatment. Although avascular necrosis has been supposed as the cause for these changes, the transient nature is more likely to reflect edema [6, 7].

In the soft tissues, commonly seen changes are early (edema and inflammation) and late (fibrosis) effects of radiation therapy. Especially the early effects are easily identified because of the linear margins reflecting the radiation portals. The signal intensities of hematoma (high signal intensity of methemoglobin on T1- and fluid-sensitive sequences) and hygroma (low signal intensity on T1 and high signal on fluid-sensitive sequences) allow an easy diagnosis. Follow-up imaging (also with US) and Gd-chelate-enhanced imaging are useful in excluding tumor nodules within or surrounding these postsurgical changes. Denervated muscle is easily recognized as a high signal muscle on fluid-sensitive sequences (early edema) or high signal intensity muscle on T1-weighted sequences (late atrophy).

26.3 Monitoring Response to Therapy

With some exceptions, most soft tissue tumors, and especially sarcomas, are treated with resection. Resection is often supplemented by neoadjuvant (presurgical) chemotherapy, radiation therapy before or following resection, and adjuvant chemotherapy (postsurgical). In addition trials with chemoradiation have shown promising results [8]. In contrast to chemotherapy protocols, there is still debate about the optimal use of radiation therapy as an adjunct to surgery. There are advantages and disadvantages for both pre- and postoperative scheduling of radiation. For imaging it is important to realize that the effect of radiation therapy takes at least 4 weeks to happen. Many histological changes including necrosis, liquefaction, hemorrhage, hyalinization, angiogenesis, and fibrosis occur secondary to radiation and complicate image interpretation.

Volume measurements have been proven to be insufficient (with the exception of myxoid liposarcoma) in monitoring response to radiation therapy [9–12]. Likewise tumor volume measurements are inaccurate in monitoring response to (neo)adjuvant chemotherapy and chemoradiation. Tumor biology in sarcomas is normally heterogeneous and in addition changes over time, even without therapy. Volume measurements do not capture the complicated spontaneous and therapy-induced changes within the sarcomas.

The revised RECIST 1.1 criteria originate from the era of cytotoxic chemotherapy [13]. Nowadays and even more so in the future, targeted therapies will use tumor-specific pathways to modify tumor progression, vasculature, and growth. This requires matching imaging techniques to monitor response. The EORTC soft tissue and bone sarcoma group proposed a histological grading system based on the amount of viable (also called stainable) tumor relative to necrosis. Grades are from A (no stainable tumor cells) to E (>50 % stainable tumor cells). Relationships between this new grading system and prognosis or outcome have yet to be determined. In this chapter we therefore still use the value of <10 % viable tumor to indicate good response. Compared to the older system of less than 10 % of viable tumor as a cutoff value for good response, this new system has, apart from grade A, also grade B (single or clusters of stainable tumor cells <1 % of whole specimen) and grade C 1–10 % stainable tumor cells [10].

The PERCIST criteria are a step forward for imaging evaluation because they include metabolic information visualized by FDG-PET imaging [13]. Especially with the advent of various mechanisms of chemotherapy that change tumor biology, we need to make use of an integrated approach using functional parameters obtained with multiple imaging techniques including MR (angiogenesis, membrane integrity, hypoxia, etc.) and PET [14–17]. This approach of tumor profiling has been described as radiomics [17]. For this chapter a survey of this futuristic approach is beyond our scope. In this chapter we'll briefly describe currently available clinical approaches.

Changes in tumor volume assessed with MR are also not very accurate in defining response. Only an increase in tumor volume not caused by massive hemorrhage within the tumor correlates with a poor histologic response. An unchanged or decreasing tumor volume is not predictive of a good response.

Gd-chelate-enhanced MR imaging improves identification of viable components within the tumor [14, 18]. However, static contrast-enhanced MR images are not sufficiently specific to differentiate viable tumor from early immature granulation tissue, neovascularity in necrotic areas, and reactive hyperemia. Also, static Gd-chelate-enhanced imaging results in an overestimation of the volume of residual viable tumor because the small molecular agent Gd-chelate passes from the intravascular space to the interstitium outside the tumor [18, 19]. Fast or dynamic contrast-enhanced (DCE) MRI reflects angiogenesis, in particular flow, permeability, and interstitial pressure and is thus more accurate in identifying and localizing residual viable tumor after chemotherapy thereby improving differentiation between good and poor respondents (Figs. 26.1 and 26.2). Details of this technique are presented in Chap. 5.

Therapy-induced changes in capillary permeability (time-intensity curve analysis, quantification of Ktrans) and vascular density (maximal enhancement) are often observed before changes in tumor volume. Direct visual inspection of the (subtraction) images before and after chemotherapy allows easy detection of highly vascular and/or highly perfused viable tumor tissue. Alternatively parametric analysis (see Chap. 5) using dedicated software can be used [19, 20]. When more than 10 % of the total tumor volume enhances early (defined as enhancement within 6 s after arterial enhancement), a poor response with more than 10 % of tumor tissue remaining viable should be suspected. Several pitfalls have to be avoided. Young granulation tissue at the margins of necrotic tumor may enhance early. Arterioles or small physeal vessels enhance early as well. Spatial resolution is a limitation. Tumor nests smaller than 3–5 mm^2 cannot be depicted.

Diffusion-weighted MR imaging with high b-values has potential in assessing the chemotherapeutic response of soft tissue sarcoma [12, 15, 21–23].

An increase in diffusion reflected by increasing apparent diffusion coefficient (ADC) values of sarcoma after chemotherapy corresponds to cell death (disintegration of cell membranes) and reduction in tumor cell density. Early response to chemotherapy may, however, result in a decrease of diffusion caused by dehydration, congestion, and decreased capillary permeability. It is still unclear which method of determining changes of ADC values over time is appropriate for soft tis-

sue sarcoma. Increase of the minimum ADC value seems to correlate better with good response than increase of the average ADC ratios [21].

The value of color Doppler ultrasonography with spectral analysis has been demonstrated in patients with bone and soft tissue sarcomas as long as there is a soft tissue mass. Blood flow parameters that can be measured by spectral analysis include peak velocity, mean velocity, volume flow rate, pulsatility index, and resistive index ([peak systolic velocity/end-diastolic velocity]/peak systolic velocity) [18, 24, 25]. Response to neoadjuvant chemotherapy can be reliably predicted after two cycles, but not sooner. In a good respondent, a vascular tumor with low vascular resistive index in feeding arteries changes into a system with an increased or even normalized resistive index and decreased flow and shunting in the tumor. In good respondents, the resistive indices calculated in the tumor-
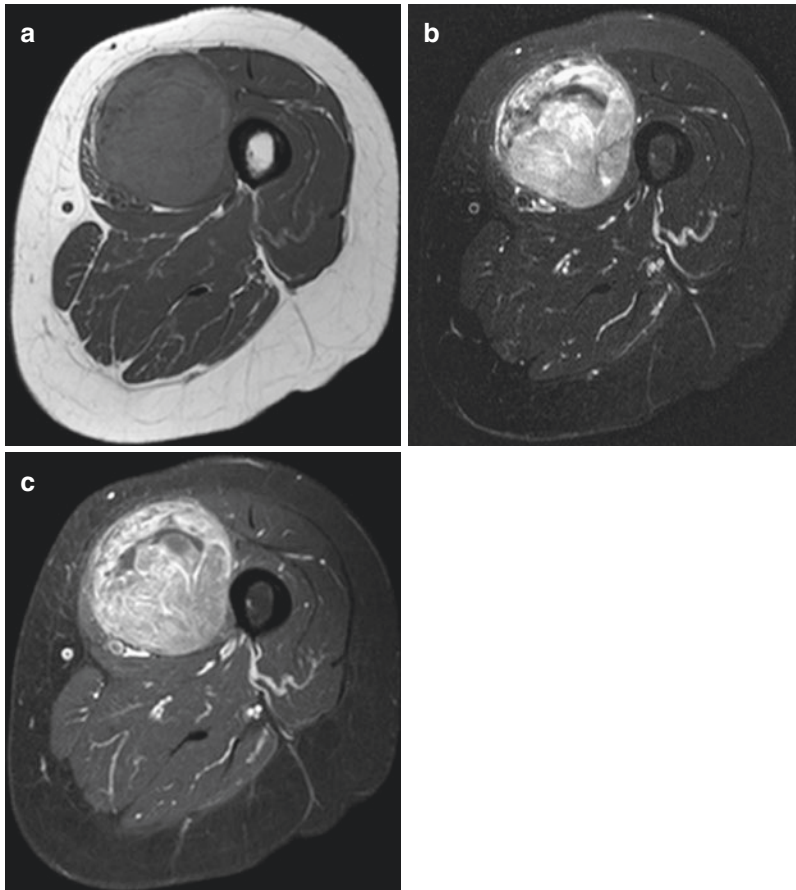

Fig. 26.1 Adult patient with synovial sarcoma medial to the femur with central necrosis diagnosed on the resected specimen. T1- (**a**) and T2-weighted frequency-selected fat-suppressed (**b**) and T1 fat-suppressed Gd-enhanced static (**c**) axial images show the tumor with centrally less enhancement. On this panel parametric images (**d**) obtained during dynamic Gd-enhanced data acquisition with a temporal resolution of 3 s and processed with ISP software package (Philips) are displayed. *Upper left* is one of the enhanced images, *upper middle* the electronically subtracted image, *upper right* time to peak, and *lower right* the wash-in rate. Below the images, a time-intensity curve is exhibited (horizontal axis time, vertical axis relative signal intensity). Artery, viable, and necrotic tumors are labeled. Following neoadjuvant chemotherapy, the same parameters are displayed (**e**). Note that the necrotic central area has increased (subtraction images), the time to peak has become longer, and the wash-in rate has decreased. Following resection the patient had a recurrent mass which has high signal intensity and fluid-fluid levels on the T2 fat-suppressed image (**f**), and on the static Gd-enhanced images (**g**), no central enhancement is observed. On the parametric images (**h**), no enhancement is observed on all parametric images nor on the time-intensity curve. A large hematoma without viable tumor was evacuated
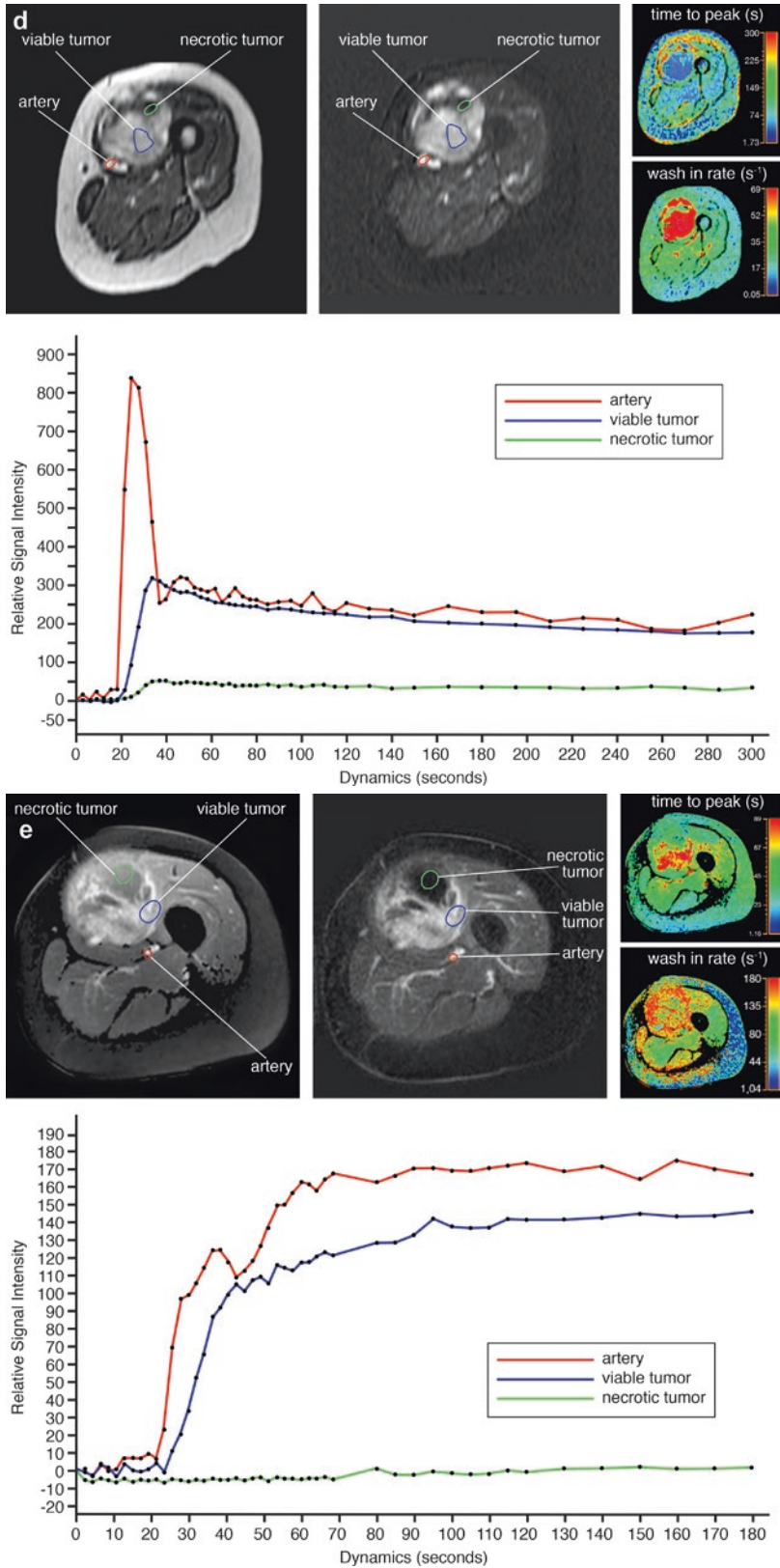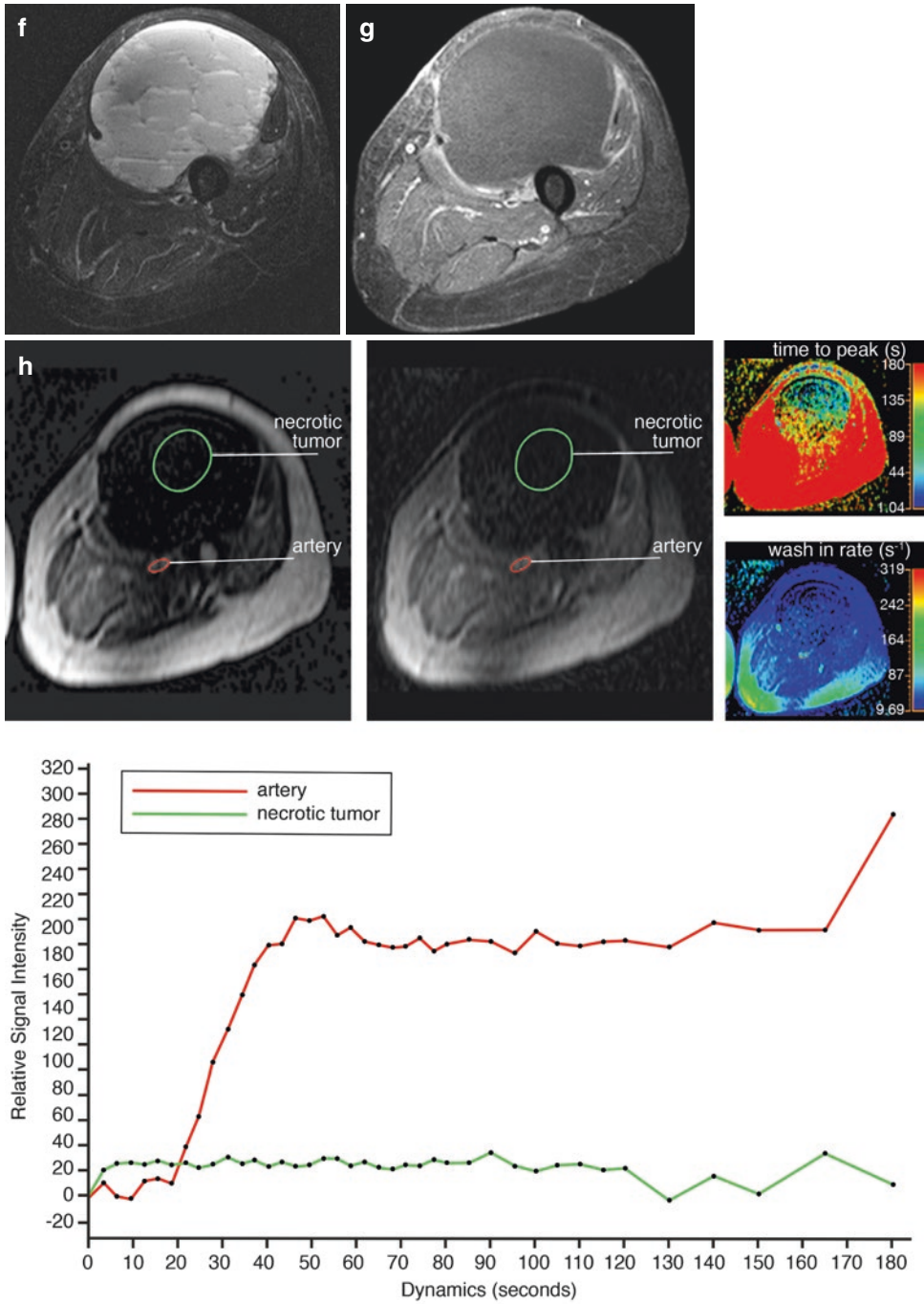
Fig. 26.1 (continued)

Fig. 26.1 (continued)

feeding artery are almost equal to the resistive indices in the contralateral reference artery. Apparently, increase of peripheral resistance corresponds to the reduction or disappearance of intratumoral high-velocity Doppler shifts, which indicates the reduced need for attracting blood from the host's circulation in chemotherapy-sensitive tumors [26].

Early studies demonstrate the potential of Doppler ultrasonography with microbubble-

based contrast agents in evaluating tumor response to chemotherapy. A decrease of contrast uptake the day after isolated limb perfusion with high-dose chemotherapy and tumor necrosis factor has been reported to correlate with a favorable histologic response. No ultrasound parameters have been reported that can predict the response to therapy before the start of treatment.

There have been conflicting reports on the usefulness of glucose metabolism imaged by 18F-deoxyglucose positron emission tomography (18F-FDG-PET) as a parameter to assess response to chemotherapy in sarcoma [27]. Following chemotherapy, the standardized uptake value (SUV) decreases. Most studies report a larger decrease of SUVmax in responders as opposed to nonresponders [28–33]. Most studies are in heterogeneous populations of bone and soft tissue sarcoma. It seems that metabolic tumor volumes are a better target than SUVmax values. Differences in metabolic volume, defined as the number of voxels within the volume of interest that have an uptake greater than that of the chosen background threshold, have been reported to correlate better with response [29]. This tumor component correlates with the viable tumor as defined by early enhancement on DCE MRI and seems a promising venue of further research.

With the advent of insights in analyzing metabolic tumor volume or residual viable tumor using various SUV parameters and the rise of reliable commercial software packages to quantify DCE MRI, it is too early to define the clinical role of these techniques [27]. For the time being, we still rely on DCE MRI in combination with high-resolution MR to monitor response and, at the same time, to identify viable tumor nests before surgery. It is likely that with the advent of targeted
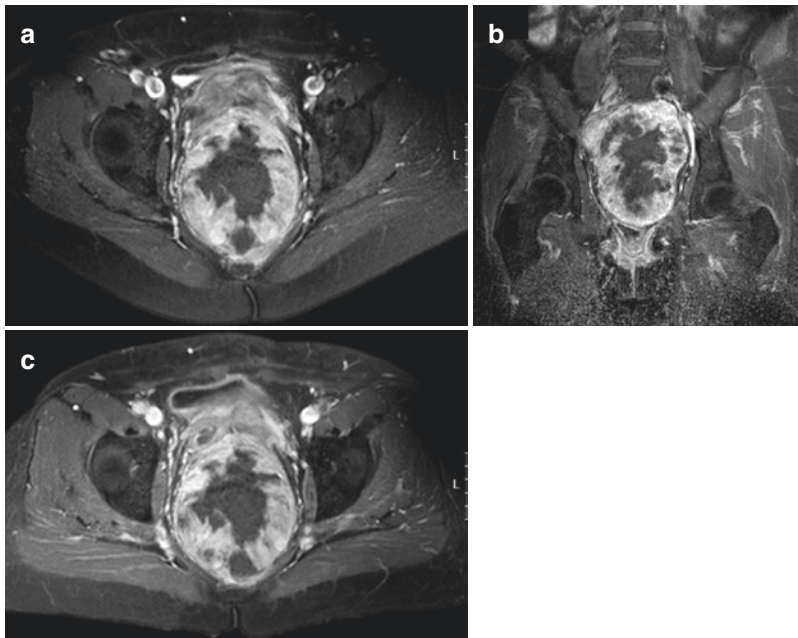

Fig. 26.2 A 64-year-old patient with solitary fibrous tumor; following presurgical radiation therapy, 50 % of the tumor was necrotic. Axial (**a**) and coronal (**b**) Gd-chelate-enhanced fat-suppressed T1-weighted images show the tumor in the pelvis. Enhancement is mainly seen in the periphery. Following radiation therapy (**c**), little change is seen on the axial fat-suppressed Gd-enhanced static image. On this panel parametric images (**d**) obtained during dynamic Gd-enhanced data acquisition with a temporal resolution of 3 s and processed with ISP software package (Philips) are displayed. *Upper left* is one of the enhanced images, upper middle the electronically subtracted image, *upper right* time to peak, and *lower right* the wash-in rate. Below the images is a time-intensity curve (horizontal axis time, vertical axis relative signal intensity). Artery, viable, and necrotic tumors are labeled. Following radiation therapy, the same parameters are displayed (**e**). Note that the time-intensity curve of the peripheral enhancing part has decreased relative to the arterial curve. Time to peak has increased, while only minor change is seen for the wash-in rate
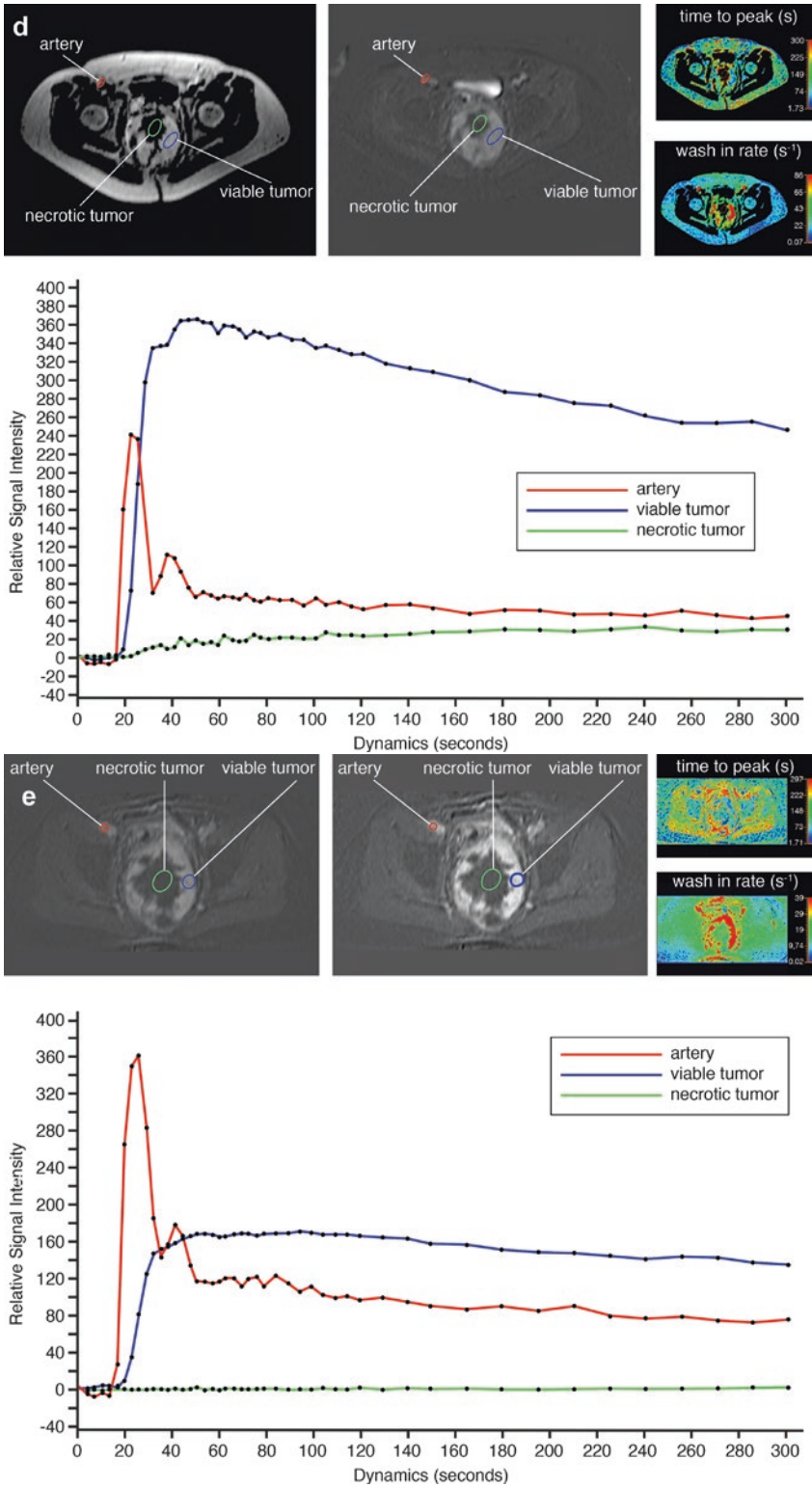
Fig. 26.2 (continued)

predominantly cytostatic, metabolic, and angio-genesis-inhibiting cancer treatments, 18F-FDG-PET will take a prominent place together with other PET tracers requiring cyclotron, DCE MRI, and ultrasonography in monitoring and guiding treatment. The combination of several techniques, displaying various characteristics of tumor pheno-type in 4D, is likely to be the future. This requires advanced automated analysis of large data sets.

26.4 Locoregional Recurrence

The benefit of early detection of local recurrence depends on the availability of therapeutic options that can prolong survival. Radical compartmental resection with or without adjuvant radiotherapy and/or chemotherapy may provide long-term sal-vage in patients with a local recurrence of soft tissue sarcoma [34]. The risk for local recurrence depends on tumor site, size, grade, and adequacy of surgical margins. Although about 2–20 % of all resections will have positive margins and thus increased risk for local recurrence, its impact on overall survival remains controversial [1, 4, 35].

Several guidelines have been recommended for the follow-up of soft tissue sarcoma consisting of a combination of clinical history, physical examination, blood tests, chest radiographs, CT, and MR imaging [36–42]. The ACR advises MR follow-up at least twice a year during the first 5 years after treatment of the primary tumor and once a year 5–10 years after treatment. The ESSR and ESMO advocate 3–4 MRs during the first 2–3 years in intermediate- or high-grade sarcomas and 2–3 MRs during the first 3 years in low-grade sar-comas. An MR once a year 5–10 years after pri-mary treatment is also advocated by ESSR [34, 43–47]. Most institutions rely on consensus-based guidelines due to the absence of evidence-based guidelines. Surveillance strategies that, through early detection and treatment, improve survival and quality of life while minimizing costs have yet to be identified in randomized clinical trials. Only few studies have been reported on the effi-cacy of surveillance strategies for the follow-up of soft tissue sarcoma [37, 38, 48]. According to Whooley et al., clinical assessment and physical examination are the most useful tools for evaluat-ing locoregional recurrence, whereas routine MR imaging of the primary tumor site and laboratory blood tests appear ineffective strategies. In a ret-rospective review of 141 patients, they detected by routine annual imaging only one asymptom-atic local recurrence; all others were found on physical examination of the primary site [37, 48]. However, MR imaging has shown to be useful in patients in whom physical examination is ham-pered due to radiotherapy changes.

When indicated, MR imaging is the most use-ful technique for identifying suspected local recurrence or residual disease after incomplete resection [34, 49]. An MR using a T2-weighted sequence with frequency-selective fat saturation or short tau inversion recovery (STIR) or Dixon sequence with water reconstruction is considered to be the most useful first step for detecting recur-rent tumor (Fig. 26.3). The morphology of the lesion and the signal intensity contribute to the definition of its character. Low signal intensity on T2-weighted images or diffuse high signal intensity on T2-weighted images excludes tumor recurrence in 99 % of patients. Mature scar tissue usually exhibits low signal intensity (Fig. 26.4) because of its fibrous tissue content, as described in previous studies. Diffuse high signal intensity with a feather-like appearance, without mass effect, generally represents post-therapy change or inflammation. High signal intensity mass-like
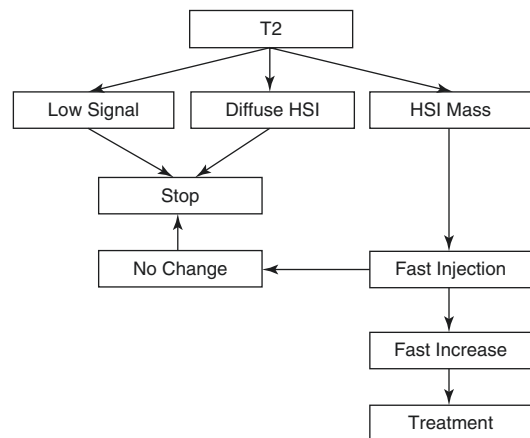

Fig. 26.3 Flowchart of MR imaging in the follow-up of aggressive soft tissue tumors

lesions on T2-weighted images require further examination with intravenous Gd-chelates [50].

Fat-suppressed T1-weighted fast spin echo sequences after Gd-chelate injection can be used to distinguish non-enhancing post-therapy hygroma, seroma, or hematoma from enhancing tumor recurrence, post-therapy fibrosis, granulation tissue, or inflammatory masses (Fig. 26.5). The T1 fat-suppressed images obtained after administration of the contrast agent should be compared to subtraction images (for instance, obtained in the dynamic sequence, see below) or to pre-contrast T1 fat-suppressed images to correct for pseudo-enhancement caused by scaling effects. Absence of contrast enhancement excludes recurrent tumor. On these standard contrast-enhanced images, the differentiation between recurrent viable tumor and post-therapy fibrosis or inflammatory pseudomasses may remain difficult. However, in these cases dynamic contrast-enhanced MR imaging may prove helpful
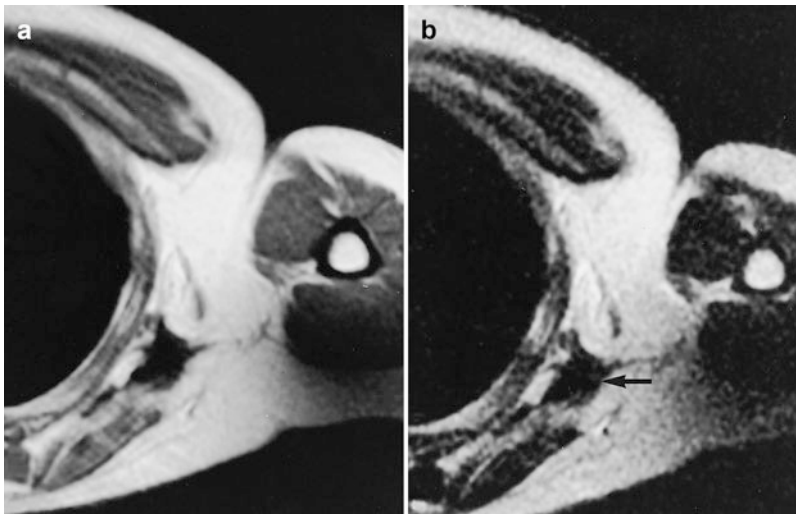

Fig. 26.4 (**a**, **b**) Malignant soft tissue tumor studied after surgery and radiotherapy in a 30-year-old male: (**a**) axial T2-weighted MR image shows low signal intensity (*arrow*) indicative of no recurrence; (**b**) the scar also has low signal on T1-weighted MR image
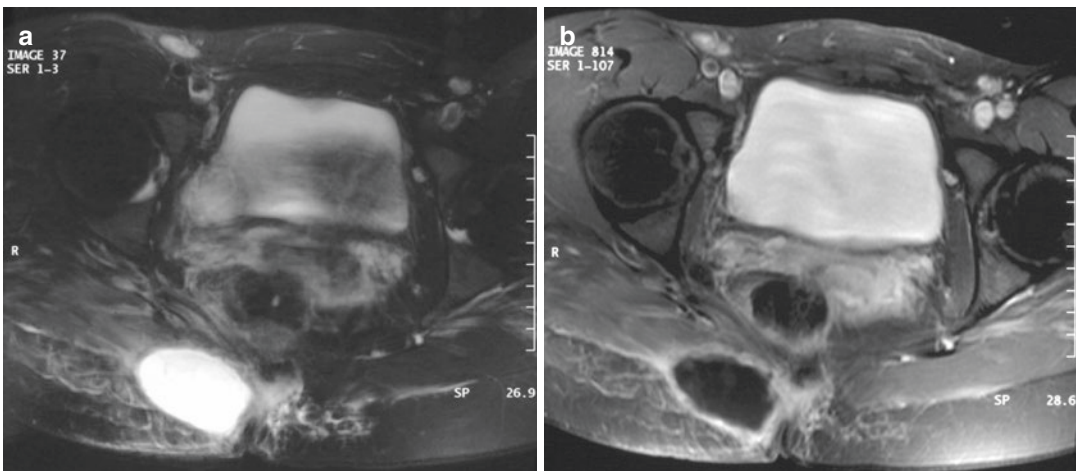

Fig. 26.5 (**a**, **b**) Three months after resection of desmoid-type fibromatosis of the pelvis in a 26-year-old female: (**a**) axial T2-weighted MR image shows a well-defined mass with homogeneous high signal intensity; (**b**) on axial fat-suppressed T1-weighted MR image after intravenous administration of gadolinium, chelate is only a small rim of enhancement seen consistent with a postoperative seroma that resolved spontaneously

[34, 51]. Dynamic contrast-enhanced MR imaging allows differentiation between inflammation and recurrent or residual tumor. After a rapid bolus injection of contrast, viable tumor exhibits rapid progressive increase of signal intensity followed by washout or plateau phase, whereas the signal from inflammatory changes will also increase but later [52] (Fig. 26.6). The exception is young granula-
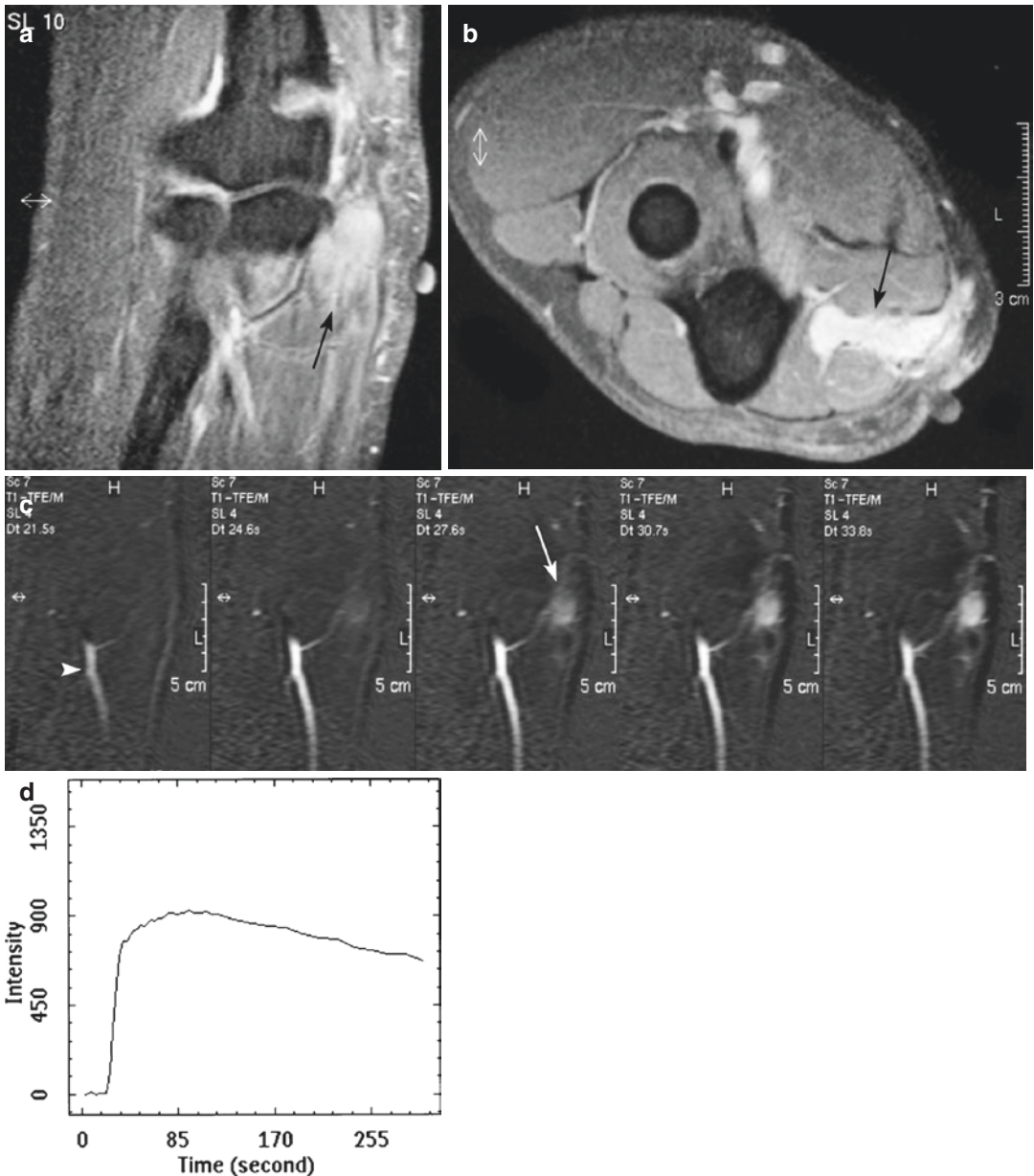

Fig. 26.6 (**a–d**) Fifteen months after resection and radiotherapy of a liposarcoma of the elbow in a 25-year-old male: (**a**, **b**) coronal and axial fat-suppressed T1-weighted MR image after gadolinium chelate shows an ill-defined homogeneous enhancing soft tissue mass (*arrow*). Markers on the skin demonstrate the surgical scar; (**c**) coronal consecutive dynamic contrast-enhanced subtraction images of the same level obtained with a temporal resolution of 3 s. Tumor enhancement (*arrow*) is seen 3 s after arrival of the bolus contrast in the artery (*arrowhead*) suggestive of tumor recurrence; (**d**) time-intensity curve of a region of interest in the soft tissue mass demonstrating rapid progressive enhancement followed by a washout phase. Histologic examination after Tru-Cut biopsy showed recurrence of liposarcoma

tion issue and reactive changes secondary to surgery or radiation within the last 6 months.

Diffusion-weighted imaging has potential in adding specificity in the diagnosis of recurrent tumor. Preliminary studies have shown a statistical difference between recurrent tumor and nonneoplastic masses secondary to earlier treatment [34, 51].

Each case of a suspicious (recurrent) mass should be treated as if it is a new sarcoma. Confirmation should be obtained by cytological sampling or core-needle (Tru-Cut or Jamshidi) biopsy after locoregional restaging by MR imaging. Histological biopsy should always be performed after MR imaging because reactive changes, hemorrhage, and edema secondary to biopsy may hamper interpretation of MR images and therefore interfere with staging.

Preliminary studies of positron emission tomography (PET) demonstrate the potential of PET with FDG as an additional tool for detecting local recurrence of soft tissue sarcoma. Moreover, PET seems particularly useful in patients with extensive histories of surgery and radiation therapy, in the setting in which MR imaging interpretation can be difficult [53, 54]. The caveat here is that a negative PET-CT can only be used to exclude recurrence, if the initial tumor accumulates sufficient FDG.

Desmoid-type fibromatoses are benign fibroblastic proliferations that arise in the deep soft tissues and are characterized by infiltrative growth in the surrounding soft tissue structures and the absence of a pseudocapsule. Because of this growth pattern, local recurrence after surgery is virtually unavoidable. Routine follow-up MR imaging of patients with desmoid-type fibromatosis seems justified not only to detect (often asymptomatic) local recurrence but also to

evaluate the natural behavior of these lesions as they change from cellular active lesions toward mature, collagenous inert lesions [55] (Fig. 26.7).
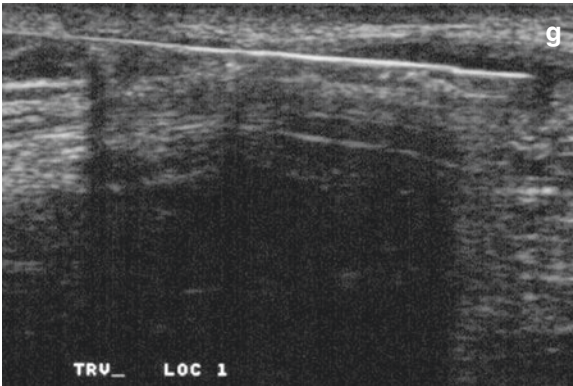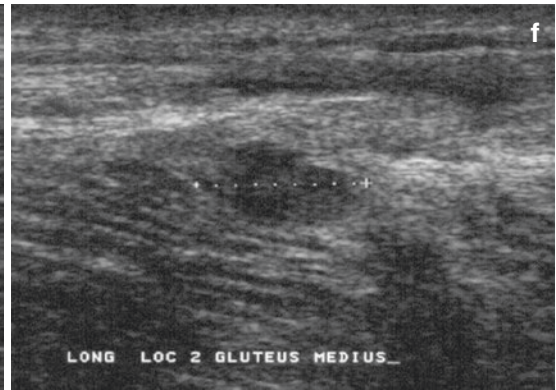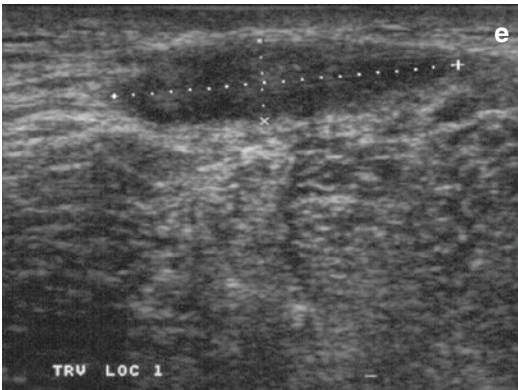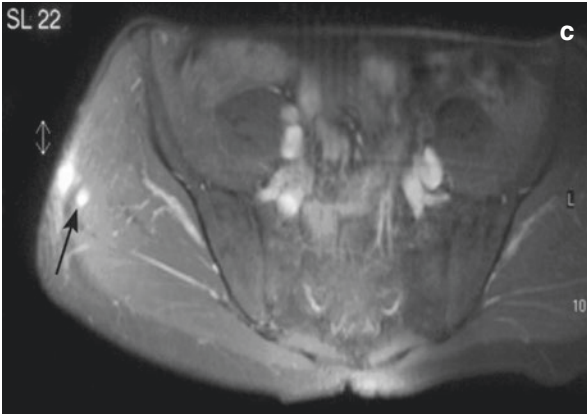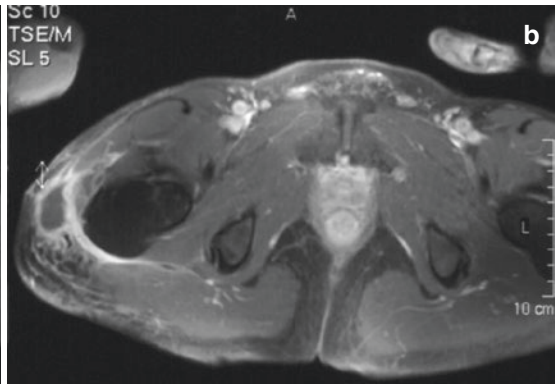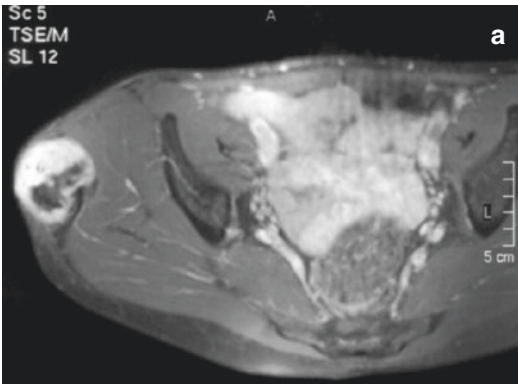
26.5   Metastases

Early detection of pulmonary metastases is an important component of surveillance because the overall survival of sarcoma patients mainly depends on the development of distant metastases (Fig. 26.8). Metastatic spread is found predominantly in the lungs, and about 70 % of all patients who develop metastases will have distant disease confined to the lungs [56]. CT is superior to PET-CT in the detection of pulmonary metastases [57].

Pulmonary metastasectomy is considered a standard practice since there is indeed a small population that can be cured. Whooley et al. studied the cost-effectiveness of chest radiograph surveillance in primary soft tissue sarcomas in a retrospective analysis. They proved the utility of chest radiograph surveillance on the basis of a review of 74 patients with first recurrence confined to the lungs (79 % of all first recurrences). Although chest CT is recommended as part of the staging evaluation for all patients with high-grade soft tissue sarcomas due to higher sensitivity than chest radiographs, the role of CT in the surveillance of metastatic disease has not been determined yet. However, extrapolations of results of chest CT at time of initial staging didn't demonstrate cost-effectiveness of routine use of surveillance chest CT over chest radiographs when the risk of pulmonary metastatic disease was low (thus in low-grade tumors) [38, 58]. However, in our practice we routinely use chest CT rather than plain films to rule out pulmonary metastases.

Fig. 26.7 (**a–g**) Desmoid-type fibromatosis in the thigh in a 47-year-old male: (**a**) axial fat-suppressed T1-weighted MR image after gadolinium chelate. The relatively well-defined soft tissue mass shows inhomogeneous enhancement. The non-enhancing area demonstrated low signal intensity on all pulse sequences; (**b**) 3 months after resection, axial fat-suppressed T1-weighted MR image after gadolinium chelate reveals a postoperative seroma; (**c**, **d**) 12 months after resection, axial and coronal fat-suppressed T1-weighted MR image after gadolinium chelate. Spontaneous regression of the postoperative seroma but appearance of new small intramuscular enhancing nodules suggestive of multifocal recurrence (*arrow*); (**e**, **f**) the nodules were identified on ultrasound as hypoechoic soft tissue masses; (**g**) ultrasound-guided histological Tru-Cut biopsy was performed and recurrence of desmoid-type fibromatosis was confirmed
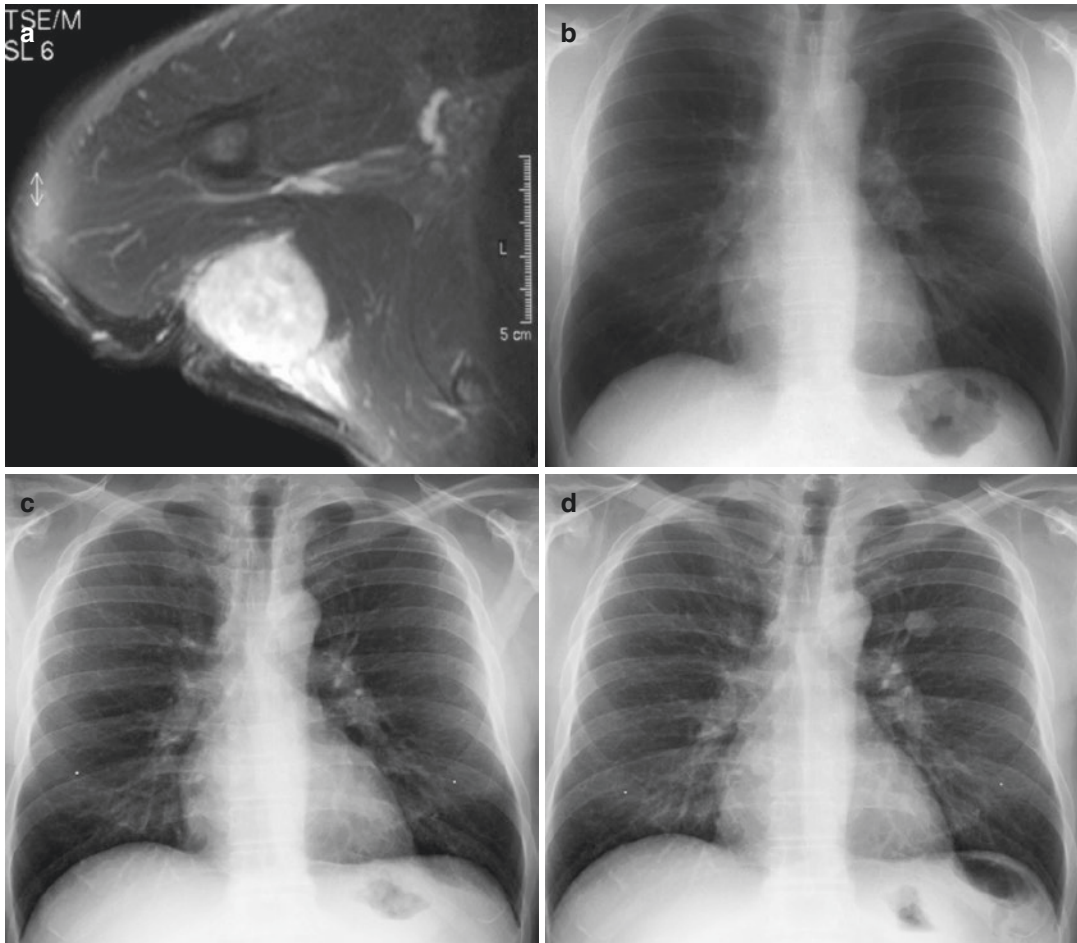
Fig. 26.8 (**a–d**) Myxofibrosarcoma of the axilla in a 42-year-old man: (**a**) fat-suppressed axial T2-weighted MR image of the axilla. Staging chest CT at time of diagnosis demonstrated no lung metastases; (**b**) 3 weeks after resection, normal chest radiograph; (**c**) 3 months after resection, normal chest radiograph; (**d**) 6 months after resection, a new solitary lung nodule in the left upper lobe is demonstrated. Metastasectomy was performed

Key Points

1. Therapy-induced changes in normal tissue can be quite extensive but can be diagnosed by combining imaging findings (morphology, location, MR signal intensities) with information on tumor therapy and supportive therapy including timing of therapeutic interventions.
2. Monitoring response of sarcomas to therapy is complicated because of spontaneous and therapy-induced change of biologic behavior of sarcomas.

Functional imaging, including dynamic Gd-chelate-enhanced MR, diffusion MR, MRS, and PET-CT, is in the process of replacing volume-based assessments such as RECIST 1.1.

3. Clinical evaluation based on attention to the clinical history (pain, swelling) and physical examination seems to be a reliable initial method in local surveillance strategies. A rational and practical surveillance algorithm should include routine office visits every 4 months for 2

years, every 6 months for 3 years, and then annually. When the initial tumor site is difficult to palpate (retroperitoneum, ENT area), when the tumor is not bulky in presentation (no pseudocapsule such as desmoid-type fibromatosis), or when there is clinical suspicion, MR imaging or PET-CT (when the initial tumor was FDG active) is indicated. In other situations the role of MR imaging is based on consensus and not on proof of added value. Most organizations advise MR imaging annually or biannually, depending on grade and margins, for the first 2–3 years. For metastases, chest radiographs or low-dose pulmonary CT is indicated. In case of local recurrence, PET-CT probably is an effective method to diagnose locoregional extent of disease.

4. MR obtained 3–6 months following local therapy may be useful in defining posttreatment situation in order to facilitate interpretation of later MR examinations.

5. CT is superior to PET-CT in detecting or excluding pulmonary metastases.

References

1. Zagars GK, Ballo MT, Pisters PW et al (2003) Prognostic factors for patients with localized soft-tissue sarcoma treated with conservation surgery and radiation therapy: an analysis of 225 patients. Cancer 97(10):2530–2543

2. Huth JF, Eilber FR (1988) Patterns of metastatic spread following resection of extremity soft-tissue sarcomas and strategies for treatment. Semin Surg Oncol 4(1):20–26

3. Gibbs JF, Lee RJ, Driscoll DL, McGrath BE, Mindell ER, Kraybill WG (2000) Clinical importance of late recurrence in soft-tissue sarcomas. J Surg Oncol 73(2):81–86

4. Lewis JJ, Leung D, Casper ES, Woodruff J, Hajdu SI, Brennan MF (1999) Multifactorial analysis of long-term follow-up (more than 5 years) of primary extremity sarcoma. Arch Surg 134(2):190–194

5. Gerrand CH, Bell RS, Wunder JS et al (2003) The influence of anatomic location on outcome in patients with soft tissue sarcoma of the extremity. Cancer 97(2):485–492

6. Karmazyn B, Cohen MD, Jennings SG, Robertson KA (2012) Marrow signal changes observed in follow-up whole-body MRI studies in children and young adults with neurofibromatosis type 1 treated with imatinib mesylate (Gleevec) for plexiform neurofibromas. Pediatr Radiol 42:1218–1222

7. Campiotti L, Codari R, Appio L, Ultori C, Solbiati F, Maria GA, Venco A (2007) Bone marrow necrosis related to imatinib mesylate therapy for cml bilineal blast crisis. Leuk Res 31:1768–1770

8. Meyer JM, Perlewitz KS, Hayden JB et al (2013) Phase I trial of preoperative chemoradiation plus sorafenib for high-risk extremity soft tissue sarcomas with dynamic contrast-enhanced MRI correlates. Clin Cancer Res 19:6902–6911

9. Roberge D, Skamene T, Nahal A et al (2010) Radiological and pathological response following pre-operative radiotherapy for soft-tissue sarcoma. Radiother Oncol 97:404–407

10. Wardelmann E, Haas RL, Bovée JV, Terrier P, Lazar A, Messiou C, LePechoux C, Hartmann W, Collin F, Fisher C, Mechtersheimer G, DeiTos AP, Stacchiotti S, Jones RL, Gronchi A, Bonvalot S (2016) Evaluation of response after neoadjuvant treatment in soft tissue sarcomas; the European Organization for Research and Treatment of Cancer-Soft Tissue and Bone Sarcoma Group (EORTC-STBSG) recommendations for pathological examination and reporting. Eur J Cancer 53:84–95. doi:10.1016/j.ejca.2015.09.021, Epub 2015 Dec 14

11. Miki Y, Ngan S, Clark JCM et al (2010) The significance of size change of soft tissue sarcoma during preoperative radiotherapy. Eur J Surg Oncol 36:678–683

12. Messiou C, Bonvalot S, Gronchi A, Vanel D, Meyer M, Robinson P, Morosi C, Bloem JL, Terrier PH, Lazar A, Le Péchoux C, Wardelman E, Winfield JM, Boulet B, Bovée J, Haas RL (2016) Evaluation of response after pre-operative radiotherapy in soft tissue sarcomas; the European Organisation for Research and Treatment of Cancer - Soft Tissue and Bone Sarcoma Group (EORTC - STBSG) and Imaging Group recommendations for radiological examination and reporting with an emphasis on magnetic resonance imaging. Eur J Cancer 56:37–44. doi:10.1016/j.ejca.2015.12.008, Epub 2016 Jan 20

13. Costelloe CM, Chuang HH, Madewell JE et al (2010) Cancer response criteria and bone metastases: RECIST 1.1, MDA and PERCIST. J Cancer 1:80–92

14. Bloem JL, Reiser MF, Vanel D (1990) Magnetic resonance contrast agents in the evaluation of the musculoskeletal system. Magn Reson Q 6:136–163

15. Li SP, Padhani AR (2012) Tumor response assessments with diffusion and perfusion MRI. J Magn Reson Imaging 35:745–763

16. Sheikhbahaei S, Marcus C, Hafezi-Nejad N, Taghipour M, Subramaniam RM (2015) Value of FDG PET/CT in patient management and outcome of skeletal and soft tissue sarcomas. PET Clin 10(3):375–393. doi:10.1016/j.cpet.2015.03.003, Epub 2015 Apr 16

17. Vallières M, Freeman CR, Skamene SR, El Naqa I (2015) A radiomics model from joint FDG-PET and MRI texture features for the prediction of lung metastases in soft-tissue sarcomas of the extremities. PET Clin 10(3):375–393. doi:10.1016/j.cpet.2015.03.003, Epub 2015 Apr 16

18. van der Woude HJ, Bloem JL, Schipper J et al (1994) Changes in tumor perfusion induced by chemotherapy in bone sarcomas: color Doppler flow imaging compared with contrast-enhanced MR imaging and three-phase bone scintigraphy. Radiology 191:421–431

19. Verstraete KL, De Deene Y, Roels H et al (1994) Benign and malignant musculoskeletal lesions: dynamic contrast-enhanced MR imaging—parametric "first-pass" images depict tissue vascularization and perfusion. Radiology 192:835–843

20. Egmont-Petersen M, Hogendoorn PC, van der Geest RJ et al (2000) Detection of areas with viable remnant tumor in postchemotherapy patients with Ewing's sarcoma by dynamic contrast-enhanced MRI using pharmacokinetic modeling. Magn Reson Imaging 18: 525–535

21. Oka K, Yakushiji T, Sato H et al (2010) The value of diffusion-weighted imaging for monitoring the chemotherapeutic response of osteosarcoma: a comparison between average apparent diffusion coefficient and minimum apparent diffusion coefficient. Skeletal Radiol 39:141–146

22. Schnapauff D, Zeile M, Niederhagen MB et al (2009) Diffusion-weighted echo-planar magnetic resonance imaging for the assessment of tumor cellularity in patients with soft-tissue sarcomas. J Magn Reson Imaging 29:1355–1359

23. Padhani AR, Liu G, Koh D-M et al (2009) Diffusion-weighted magnetic resonance imaging as a cancer biomarker: consensus and recommendations. Neoplasia 11:102–125

24. Taylor GA, Perlman EJ, Scherer LR et al (1991) Vascularity of tumors in children: evaluation with color Doppler imaging. AJR Am J Roentgenol 157: 1267–1271

25. Kiessling F, Krix M, Heilmann M et al (2003) Comparing dynamic parameters of tumor vascularization in nude mice revealed by magnetic resonance imaging and Doppler sonography. Invest Radiol 38:516–524

26. van der Woude HJ, Bloem JL, van Oostayen JA et al (1995) Treatment of high-grade bone sarcomas with neoadjuvant chemotherapy: the utility of sequential color Doppler sonography in predicting histopathologic response. AJR Am J Roentgenol 165:125–133

27. Becher S, Oskouei S (2015) Pet imaging in sarcoma. Orthop Clin North Am. 46(3):409–415, xi. doi:10.1016/j.ocl.2015.03.001. Epub 2015 Apr 11

28. Benz MR, Tchekmedyian N, Eilber FC et al (2009) Utilization of positron emission tomography in the management of patients with sarcoma. Curr Opin Oncol 21:345–351

29. Gaston LL, Di Bella C, Slavin J et al (2011) 18F-FDG PET response to neoadjuvant chemotherapy for Ewing sarcoma and osteosarcoma are different. Skeletal Radiol 40:1007–1015. Nucl Med Rev Cent East Eur. 2016;19(1):22–27. doi:10.5603/NMR.2016.0005

30. Dancheva Z, Bochev P, Chaushev B, Yordanova T, Klisarova A (2015) Dual-time point 18FDG-PET/CT imaging may be useful in assessing local recurrent disease in high grade bone and soft tissue sarcoma. Phys Med Biol 60(14):5471–5496. doi:10.1088/0031-9155/60/14/5471, Epub 2015 Jun 29

31. Vallières M, Freeman CR, Skamene SR, El Naqa I (2015) A radiomics model from joint FDG-PET and MRI texture features for the prediction of lung metastases in soft-tissue sarcomas of the extremities. Clin Imaging 39(5):866–870. doi:10.1016/j.clinimag.2015.05.014, Epub 2015 Jun 3

32. Schuler MK, Platzek I, Beuthien-Baumann B, Fenchel M, Ehninger G, van den Hoff J (2015) (18)F-FDG PET/MRI for therapy response assessment in sarcoma: comparison of PET and MR imaging results. Clin Imaging 39(5):866–870

33. Hongtao L, Hui Z, Bingshun W et al (2012) 18F-FDG positron emission tomography for the assessment of histological response to neoadjuvant chemotherapy in osteosarcomas: a meta-analysis. Surg Oncol 21: e165–e170

34. Noebauer-Huhmann IM, Weber MA, Lalam RK, Trattnig S, Bohndorf K, Vanhoenacker F, Tagliafico A, van Rijswijk C, Vilanova JC, Afonso PD, Breitenseher M, Beggs I, Robinson P, de Jonge MC, Krestan C, Bloem JL (2015) Soft tissue tumors in adults: ESSR-approved guidelines for diagnostic imaging. Semin Musculoskelet Radiol 19(5), e1. doi:10.1055/s-0036-1572350.Epub2016Feb

35. Singer S, Antman K, Corson JM, Eberlein TJ (1992) Long-term salvageability for patients with locally recurrent soft-tissue sarcomas. Arch Surg 127(5): 548–553

36. Trovik CS, Bauer HC, Alvegard TA et al (2000) Surgical margins, local recurrence and metastasis in soft tissue sarcomas: 559 surgically-treated patients from the Scandinavian Sarcoma Group Register. Eur J Cancer 36(6):710–716

37. Whooley BP, Gibbs JF, Mooney MM, McGrath BE, Kraybill WG (2000) Primary extremity sarcoma: what is the appropriate follow-up? Ann Surg Oncol 7(1):9–14

38. Kane JM III (2004) Surveillance strategies for patients following surgical resection of soft tissue sarcomas. Curr Opin Oncol 16(4):328–332

39. Patel SR, Zagars GK, Pisters PW (2003) The follow-up of adult soft-tissue sarcomas. Semin Oncol 30(3):413–416

40. Beitler AL, Virgo KS, Johnson FE, Gibbs JF, Kraybill WG (2000) Current follow-up strategies after potentially curative resection of extremity sarcomas: results of a survey of the members of the society of surgical oncology. Cancer 88(4):777–785

41. Davies AM, Vanel D (1998) Follow-up of musculoskeletal tumors. I Local recurrence. Eur Radiol 8(5):791–799

42. Goel A, Christy ME, Virgo KS, Kraybill WG, Johnson FE (2004) Costs of follow-up after potentially curative treatment for extremity soft-tissue sarcoma. Int J Oncol 25(2):429–435

43. National Guideline Clearinghouse. ACR Appropriateness Criteria® follow-up of malignant or aggressive musculoskeletal tumors. Available from: http://www.guideline.gov/content.aspx?id=32617

44. Grobmyer SR, Brennan MF (2003) Predictive variables detailing the recurrence rate of soft tissue sarcomas. Curr Opin Oncol 15(4):319–326

45. Cancer Research UK. Follow up for soft tissue sarcoma. Available from: http://www.cancerresearchuk.org/about-cancer/type/sarcoma/treatment/follow-up-for-soft-tissue-sarcoma

46. AMSOS (2015) Austrian Musculoskeletal Oncology Society. http://www.amsos.at

47. ESMO/European Sarcoma Network Working Group (2014) Soft tissue and visceral sarcomas: ESMO Clinical Practice Guidelines for diagnosis, treatment and follow-up. Ann Oncol 25(Suppl 3):iii102–iii112

48. Whooley BP, Mooney MM, Gibbs JF, Kraybill WG (1999) Effective follow-up strategies in soft tissue sarcoma. Semin Surg Oncol 17(1):83–87

49. Vanel D, Lacombe MJ, Couanet D, Kalifa C, Spielmann M, Genin J (1987) Musculoskeletal tumors: follow-up with MR imaging after treatment with surgery and radiation therapy. Radiology 164(1):243–245

50. Panicek DM, Schwartz LH, Heelan RT, Caravelli JF (1995) Non-neoplastic causes of high signal intensity at T2-weighted MR imaging after treatment for musculoskeletal neoplasm. Skeletal Radiol 24(3):185–190

51. Del Grande F, Subhawong T, Weber K, Aro M, Mugera C, Fayad LM (2014) Detection of soft-tissue sarcoma recurrence: added value of functional MR imaging techniques at 3.0 T. Radiology 271(2):499–511

52. Vanel D, Shapeero LG, Tardivon A, Western A, Guinebretiere JM (1998) Dynamic contrast-enhanced MRI with subtraction of aggressive soft tissue tumors after resection. Skeletal Radiol 27(9):505–510

53. Kole AC, Nieweg OE, van Ginkel RJ et al (1997) Detection of local recurrence of soft-tissue sarcoma with positron emission tomography using [18F]fluorodeoxyglucose. Ann Surg Oncol 4(1):57–63

54. Johnson GR, Zhuang H, Khan J, Chiang SB, Alavi A (2003) Role of positron emission tomography with fluorine-18-deoxyglucose in the detection of local recurrent and distant metastatic sarcoma. Clin Nucl Med 28(10):815–820

55. Vandevenne JE, De Schepper AM, De Beuckeleer L et al (1997) New concepts in understanding evolution of desmoid tumors: MR imaging of 30 lesions. Eur Radiol 7(7):1013–1019

56. Billingsley KG, Lewis JJ, Leung DH, Casper ES, Woodruff JM, Brennan MF (1999) Multifactorial analysis of the survival of patients with distant metastasis arising from primary extremity sarcoma. Cancer 85(2):389–395

57. Dancheva Z, Bochev P, Chaushev B, Yordanova T, Klisarova A (2016) Dual-time point 18FDG-PET/CT imaging may be useful in assessing local recurrent disease in high grade bone and soft tissue sarcoma. Nucl Med Rev Cent East Eur 19(1):22–27. doi:10.5603/NMR.2016.0005

58. Fleming JB, Cantor SB, Varma DG et al (2001) Utility of chest computed tomography for staging in patients with T1 extremity soft tissue sarcomas. Cancer 92(4):863–868